Gln^{212}, Asn^{270}, and Arg^{301} Are Critical for Catalysis by Adenylosuccinate Lyase from *Bacillus subtilis*†

Mark L. Segall and Roberta F. Colman*

Department of Chemistry and Biochemistry, University of Delaware, Newark, Delaware 19716

Received March 16, 2004; Revised Manuscript Received April 20, 2004

ABSTRACT: In adenylosuccinate lyase from *Bacillus subtilis*, Gln^{212}, Asn^{270}, and Arg^{301} are conserved and located close to the succinyl moiety of docked adenylosuccinate. We constructed mutant enzymes with Gln^{212} replaced by Glu and Met, Asn^{270} by Asp and Leu, and Arg^{301} by Gln or Lys. The wild-type and mutant enzymes were expressed in *Escherichia coli* and purified to homogeneity. The specific activities of the Q212M and the 270 and 301 mutant enzymes were decreased more than 3000-fold as compared to the wild type. Only Q212E retained sufficient activity for determination of its kinetic parameters: V_{max} was decreased ∼1000-fold, and K_m was increased 6-fold, as compared to the wild-type enzyme. Adenylosuccinate binding studies of the other mutants revealed greatly weakened affinities that contributed to, but did not account entirely for, the loss of activity. These mutant enzymes did not differ greatly from the wild-type enzyme in secondary structure or subunit association state, as shown by circular dichroism spectroscopy and light-scattering photometry. Incubation of pairs of inactive mutant enzymes led to reconstitution of some functional sites by subunit complementation, with recovery of up to 25% of the specific activity of the wild-type enzyme. Subunit complementation occurs only if the two mutations are contributed to the active site by different subunits. Thus, mixing Q212E with N270L enzyme yielded a specific activity of ∼20% of the wild-type enzyme, while mixing Q212M with R301K enzyme did not restore activity. As supported by computer modeling, the studies presented here indicate that Gln^{212}, Asn^{270}, and Arg^{301} are indispensable to catalysis by adenylosuccinate lyase and probably interact noncovalently with the carboxylate anions of the substrates 5-aminoimidazole-4(*N*-succinylocarboxamide)ribonucleotide and adenylosuccinate, optimizing their bound orientations.

Adenylosuccinate lyase (ASL)[1] catalyzes two steps in the biosynthetic pathway of purine nucleotides: the cleavage of 5-aminoimidazole-4(*N*-succinylocarboxamide)ribonucleotide (SAICAR) to produce 5-aminoimidazole-4-carboxamide ribonucleotide (AICAR) and fumarate, and the cleavage of adenylosuccinate (SAMP) to produce AMP and fumarate (*1*). Widely distributed among living organisms, dysfunction of this enzyme in humans because of point mutations results in adenylosuccinate lyase deficiency, a disease characterized by psychomotor retardation with autistic features, epilepsy, and muscle wasting (*2*−*6*). The mutations that cause this disease are located at various regions of the enzyme, and several have been shown to affect its structural stability rather than its catalytic properties (*7*, *8*).

ASL is a member of the fumarase superfamily of enzymes. Other members include the class II fumarases (*9*), aspartase (*10*), argininosuccinate lyase (*11*, *12*), and δ-crystallin (*13*). Similar to ASL, each of these enzymes catalyzes β-elimination reactions, yielding fumarate as one of the products. The three-dimensional structures are clearly similar among enzymes of this family, although sequence identity is low (less than 25%), except for three conserved regions comprising residues 93−100, 138−147, and 261−275 in ASL from *Bacillus subtilis*, in which many residues are completely conserved across the superfamily (*14*, *15*).

X-ray crystallographic studies on ASL from *Thermotoga maritima* have revealed a homotetrameric structure (*16*), with each subunit consisting of 431 amino acids, folded into three separate structural domains. Four active site clefts are present per ASL tetramer, each located in a region where three distinct subunits come into contact (*16*). Intersubunit complementation studies have shown that each of these three subunits contributes one or more amino acid residues to the active site (*14*, *15*, *17*).

The ASL-catalyzed conversion of adenylosuccinate to AMP and fumarate proceeds via a uni-bi mechanism, where fumarate is released from the active site prior to AMP (*18*). The chemical mechanism was proposed as a β-elimination (*1*, *19*), in which one of the hydrogens attached to the β carbon of the succinyl moiety is abstracted by a general base; a double bond forms between the β and α carbon of the succinyl moiety; the leaving group is protonated at either the N1 or N6 position by a general acid; and the bond between the α carbon and N6 of the adenosine ring system of the leaving group is cleaved. As a result of affinity labeling

† This work was supported by NIH Grant 1-RO1-DK 60504.

* To whom correspondence should be addressed. Phone: (302) 831-2793. Fax: (302) 831-6335. E-mail: rfcolman@chem.udel.edu.

[1] Abbreviations: ASL, adenylosuccinate lyase; SAMP, adenylosuccinate; SAICAR, 5-aminoimidazole-4(*N*-succinylocarboxamide)ribonucleotide; AICAR, 5-aminoimidazole-4-carboxamide ribonucleotide; CD, circular dichroism; HEPES, *N*-(2-hydroxyethyl)piperazine-*N*′-2-ethanesulfonic acid.

10.1021/bi0494774 CCC: $27.50
Published on Web 05/21/2004

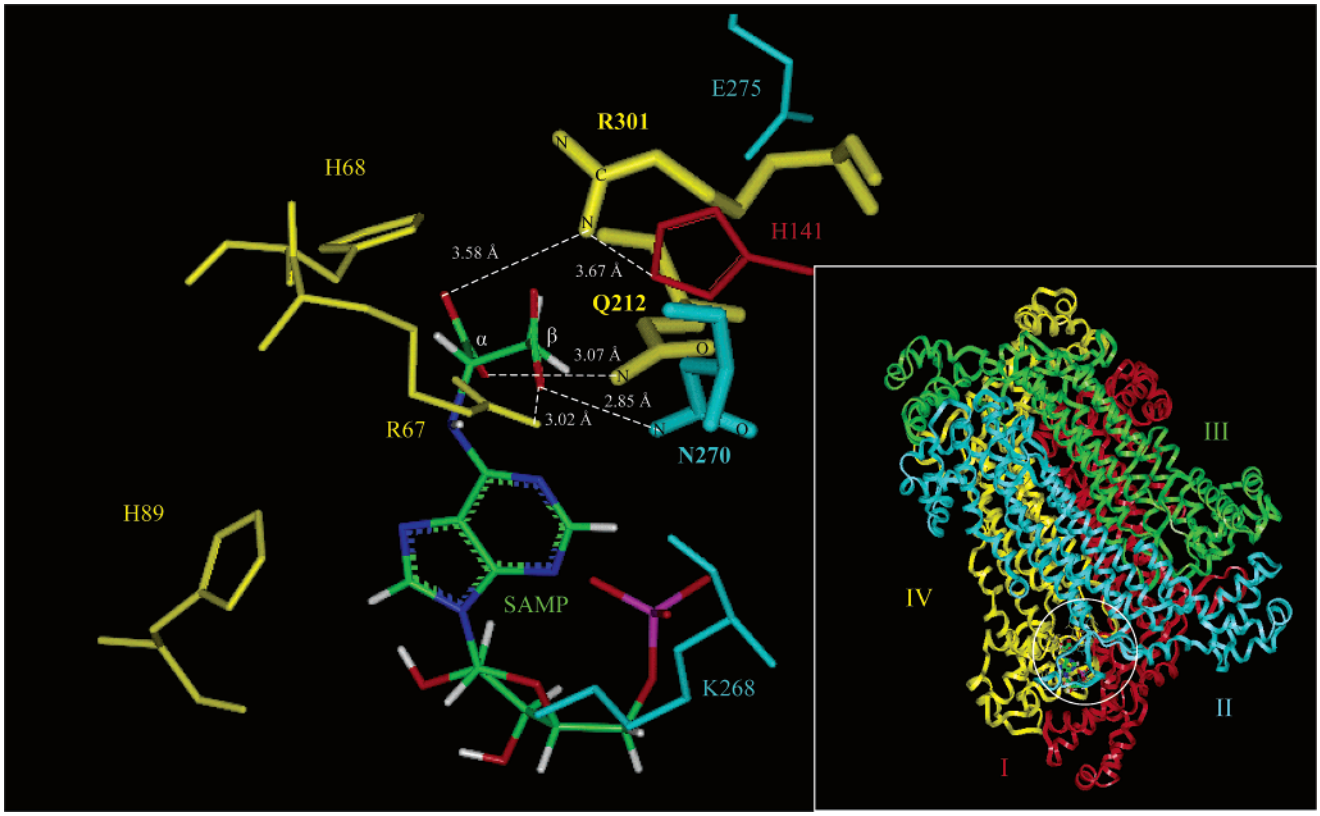

FIGURE 1: Energy-minimized model of adenylosuccinate bound to the active site of wild-type ASL. SAMP (shown in "sticks") is colored according to each atom, and each amino acid residue of ASL identified previously (also in "sticks"), as well as those that are the subject of the present study (shown in thicker "sticks" and labeled in bold type), is colored red, aqua, and yellow to denote separate subunits of origin. The α carboxylate of the succinyl moiety of SAMP is that which is closer to the N6 of the purine moiety, while the *β* carboxylate is further from N6. Only the side chains of the enzyme active-site residues are shown for clarity. Distances between carboxylate oxygens on the succinyl moiety of SAMP and non-hydrogen atoms on R67, Q212, N270, and R301 are shown. The inset depicts the full tetrameric enzyme with the region containing the active site (enlarged to the left) encircled. The four subunits, denoted in red, aqua, green, and yellow, are numbered I, II, III, and IV, respectively (in agreement with the numbering scheme used in ref *15*).

	Gln^{212}	**Asn^{270}**	**Arg^{301}**
B. subtilis	PIST**Q**TLQRD	GSSAMPHKR**N**PIGSENMTGMAR	WHE**R**DISHSSAERI
T. maritima	PVST**Q**VVPRD	GSSAMPHKK**N**PITCERLTGLSR	WHE**R**DISHSSVERY
E. coli	PYTT**Q**IEPHD	GSSTMPHKV**N**PIDFENSEGNLG	RWQ**R**DLTDSTVLRN
Yeast	PVTG**Q**TYSRK	GSSAMAYKR**N**PMRCERVCSLAR	WFE**R**TLDDSAIRRI
Chicken	MVTG**Q**TYSRK	GSSAMPYKR**N**PMRSERCCSLAR	WFE**R**TLDDSANRRV
Mouse	IITG**Q**TYTRK	GSSAMPYKR**N**PMRSERCCSLAR	WFE**R**TLDDSANRRI
Human	IITG**Q**TYTRK	GSSAMPYKR**N**PMRSERCCSLAR	WFE**R**TLDDSANRRI

FIGURE 2: Sequence alignment of amino acids of ASL in the regions surrounding Gln^{212}, Asn^{270}, and Arg^{301} (shown in bold) for representative species.

and site-directed mutagenesis, His^{141} and His^{68} were previously identified as the most likely residues to function as the general base and acid, respectively (*14*, *20*, *21*). More recently, Lys^{268} and His^{89} have been implicated in binding the phosphate group and the ribose hydroxyls of SAMP, respectively (*15*, *17*), and Glu^{275}, located less than 3 Å from His^{141}, has been suggested as participating in a charge relay interaction with this His residue (*15*).

In ASL from *B. subtilis*, Gln^{212}, Asn^{270}, and Arg^{301} are located close to the succinyl moiety of SAMP when docked into the active site (Figure 1). These residues are conserved in ASLs from *B. subtilis*, *T. maritima*, *Escherichia coli*, yeast, chicken, mouse, and human, as illustrated in Figure 2, and in fact, are conserved in the enzymes (or putative enzymes) from more than 120 species. These three residues may participate in catalysis by ASL, possibly by coordinating and/or orienting the succinyl region of the substrate. The aim of the present study was to explore the possible catalytic roles of these three amino acids through site-directed mutagenesis. Gln^{212} was replaced by Glu and Met, Asn^{270} was replaced by Asp and Leu, and Arg^{301} was substituted by Gln and Lys. Here, we describe the kinetic and biophysical characterization of these six mutant enzymes with respect to wild-type ASL. In addition, molecular modeling of each mutant enzyme, in comparison to the wild-type enzyme, was used to enhance our understanding of the effects of these amino acid replacements on the structure of the active site. A preliminary version of this work has been presented (*22*).

EXPERIMENTAL PROCEDURES

Materials. Adenylosuccinate, imidazole, and HEPES were obtained from Sigma. Oligonucleotide primers for site-directed mutagenesis and sequencing were provided by BioSynthesis. SAICAR was previously synthesized from AICAR enzymatically (*7*). The concentrated protein assay reagent was from BioRad. All other chemicals were of reagent grade.

Site-Directed Mutagenesis. The pBHis plasmid containing *B. subtilis ASL* was a generous gift from Dr. Jack E. Dixon (University of Michigan). Mutations to this gene were constructed using the Stratagene QuikChange mutagenesis kit and the pBHis plasmid. The oligonucleotide primers and their complementary sequences used to construct the mutants are as follows: CG ATT TCC ACT GAA ACC CTT CAG CGT G (Q212E), CG ATT TCC ACT ATG ACC CTT CAG CGT G (Q212M); CG CAT AAA CGA GAT CCG ATT GGC TCT G (N270D), CG CAT AAA CGA CTG CCG ATT GGC TC (N270L); and TTA TGG CAT GAG AAA GAT ATT TCT C (R301K), TTA TGG CAT GAG CAG GAT ATT TCT C (R301Q). The underlined bases designate the mutated codon. The presence of mutations was confirmed by DNA sequencing provided by the University of Delaware Center for Agricultural Biotechnology, using an ABI Prism model 377 DNA sequencer (PE Systems).

The enzymes were expressed as His-tagged proteins in *E. coli* strain BL21(DE3) and were purified using nickel-affinity chromatography as described previously (*20*, *23*). The protein purity was confirmed by electrophoresis using a 12% polyacrylamide gel in the presence of (0.1%) sodium dodecyl sulfate (*24*), as well as by gas-phase N-terminal sequencing using an Applied Biosystems Procise protein/peptide sequence analyzer. Except where otherwise mentioned, the protein concentration was determined from the absorbance at 280 nm ($E^{1\%} = 10.6$) (*20*). All protein preparations were briefly centrifuged to remove small amounts of aggregated protein prior to concentration determination and storage. Purified protein was aliquoted and kept at −80 °C.

Kinetics of B. subtilis ASLs. Enzyme activity toward SAMP was assayed by monitoring the decrease in absorbance at 282 nm (difference extinction coefficient ($\Delta\epsilon$) between SAMP and AMP = 10 000 M^{-1} cm^{-1}) (*25*). In cases where SAMP concentrations above 100 μM were used, absorbance was monitored at 290 nm ($\Delta\epsilon = 4050$ M^{-1} cm^{-1}). Specific activity was expressed as micromoles of SAMP converted to AMP and fumarate per minute per milligram of enzyme. Assays at standard conditions were conducted in a 50 mM HEPES buffer at pH 7, with 60 μM SAMP and 8 μg/mL wild-type ASL subunits at 25 °C. For Q212M ASL, as well as the Asn[270] and Arg[301] mutants, the SAMP concentration was increased to at least 120 μM to compensate for possible increases in K_m values. Q212E enzyme was assayed at concentrations of 400−450 μg/mL, and the remaining mutant enzymes, which exhibited little or no activity, were tested at 640 − 2100 μg/mL. The enzymes were preincubated at 25 °C in a water bath for 30 min prior to the assay. K_m and V_{max} for wild-type and Q212E ASL were obtained under standard conditions with varying concentrations of SAMP using the Michaelis−Menten equation.

The activity of ASL toward SAICAR was measured by monitoring the conversion of this compound to AICAR through a decrease in absorbance at 267 nm ($\Delta\epsilon = 700$ M^{-1} cm^{-1}) (*26*). Specific activity was expressed as micromoles SAICAR converted to AICAR per minute per milligram of enzyme. For comparison of ASL activities toward SAMP and SAICAR under conditions of saturating substrate concentration, while taking into account the K_m values of wild-type ASL for SAMP and SAICAR of 2.7 and 6.4 μM (*7*), respectively, the standard assay concentration for SAMP was 60 μM and for SAICAR was 90 μM. The assay mixtures were buffered at pH 7.0 using 50 mM HEPES. Because the sensitivity of the assay with SAICAR is more than 10-fold lower than that of the assay with SAMP, concentrations of wild-type ASL of between 8 and 32 μg/mL were used. Q212E, Q212M, N270D, N270L, R301K, and R301Q ASLs were similarly assayed with SAICAR but at enzyme concentrations of about 200 μg/mL for the Q212E enzyme and up to 1100 μg/mL for the others.

Binding of SAMP by Mutant Enzymes. The binding was measured by ultrafiltration using Centricon YM-10 filtration units (Millipore). The units were prewashed with a 50 mM HEPES buffer to remove glycerol from the membrane. Mutant enzymes (30−40 μM), which had been preincubated at 25 °C for 30 min, were mixed with concentrations of SAMP ranging from 30 to 200 μM in a 50 mM HEPES buffer at pH 7. These equilibrium mixtures (800 μL) were subjected to ultrafiltration to measure the concentration of free SAMP in the filtrate (ϵ at 268 nm for SAMP = 19 300 M^{-1} cm^{-1}). The equilibrium solution was placed in the top compartment of a filtration unit and spun at 5000 rpm (at 25 °C) for about 20 min. The first 200 μL to flow through the membrane (after 5−10 min of centrifugation) was discarded, while the next 200 to 250 μL was used to measure the free SAMP concentration. The concentration of bound SAMP was determined by subtracting free SAMP from the total SAMP concentration in the equilibrium mixture. Dissociation constants for SAMP were calculated for inactive ASL mutants using the Scatchard equation, $K_d = (n - r)(L_{free})/r$, where n is the number of binding sites per enzyme subunit, r is the concentration of bound ligand divided by the concentration of enzyme subunits, and L_{free} is the concentration of free ligand. When control measurements in the absence of the enzyme were conducted, it was determined that a negligible amount of SAMP was bound to the filter under these experimental conditions.

Circular Dichroism (CD) of ASL Mutants. Far-UV CD spectra were obtained from 200 to 250 nm at 0.2-nm intervals using a Jasco J710 spectropolarimeter with a 0.1-cm cylindrical quartz cuvette. Protein samples were measured at 0.3 to 0.6 mg/mL in a 20 mM potassium phosphate buffer at pH 7, containing 20 mM potassium chloride. Prior to measurement, enzyme samples were preincubated at 25 °C for 30 min. The spectrum for each sample was averaged over five acquisitions, and the background contributed by buffer was subtracted. The protein concentration was determined by a Bradford-based protein assay (Biorad), using wild-type ASL as the protein standard (*27*). Molar ellipticities were calculated at all wavelengths by the equation $[\theta] = \theta/10nCl$, where θ is the experimentally measured ellipticity, n is the number of residues per enzyme subunit (437 including the His_6 tag), C is the molar concentration of enzyme subunits, and l is the cuvette path length.

Table 1: Kinetic Parameters for Wild-Type and Mutant Enzymes[a]

enzymes	V_{max} (± S.E.) (μmol min^{-1} mg^{-1})	K_m (± S.E.) (μM)	k_{cat} (s^{-1})	k_{cat}/K_m (M^{-1} s^{-1})
wild type	1.46 ± 0.06	2.70 ± 0.78	1.22 ± 0.06	4.52×10^5
Q212E	0.0017 ± 0.0001	16.6 ± 2.9	0.0014 ± 0.0001	$0.000\,86 \times 10^5$
N270D, R301Q[b]	0.0004	N.D.[c]	0.0003	N.D.
Q212M, N270L, R301K[d]	≤0.0003	N.D.	≤0.0003	N.D.

[a] Assays were conducted using adenylosuccinate as the substrate at 25 °C in a 50 mM HEPES buffer at pH 7. All enzymes were preincubated at this temperature in a water bath for 30 min prior to assay. K_m and V_{max} (obtained from fitting to the Michaelis−Menten equation), as well as standard error (S.E.), were computed using SigmaPlot software. [b] N270D and R301Q both had specific activities of 0.0004 μmol min^{-1} mg^{-1}. [c] N.D. = not detectable. [d] Q212M, N270L, and R301K had no detectable specific activity; the lower limit of detection is approximately 0.0003 μmol min^{-1} mg^{-1}.

Molecular Mass Determination of Mutant Enzymes. Molecular masses were obtained for wild-type and mutant ASLs using a miniDAWN laser photometer (Wyatt Technology Corp., Santa Barbara, CA). Data were collected at 690 nm and analyzed by ASTRA software for Windows (*28*). Protein samples, at a concentration of approximately 0.2 mg/mL (as determined by a Bradford-based protein assay after the light-scattering experiment), were measured in a filtered 20 mM potassium phosphate buffer at pH 7.0, containing 20 mM potassium chloride. Prior to measurement, enzyme samples were preincubated at 25 °C for 30 min.

Intersubunit Complementation of Mutant Enzymes. Pairs of mutant enzymes in a 0.1 M sodium phosphate buffer (pH 7.0) were mixed in equal volumes of 100 μL to give a final concentration of 0.7 mg/mL for each mutant. The mixture was slowly frozen at −20 °C. Subsequently, the pairs were slowly thawed at room temperature, mixed, and then incubated at 25 °C. The mixtures of mutant enzymes were assayed under standard conditions as a function of time of incubation at 25 °C until maximum activity was reached. Subunit dissociation of multimeric enzymes in sodium phosphate buffers has previously been attributed to a decrease in pH upon slow freezing (*29*). Mutant enzymes treated in this way exhibited more pronounced complementation than when simply incubated in a phosphate buffer at 25 °C, likely because of the acid-induced dissociation of the oligomer. All mutants included in each experiment were also assayed separately as controls at the same total enzyme concentration following preincubation for 30 min at 25 °C.

Docking of SAMP into ASL Homology Model with Energy Minimization. Substrate docking was performed using previously constructed SAMP and a homology model of ASL from *B. subtilis* that was based on the structure of the native *T. maritima* enzyme (PDB 1c3u), crystallized at pH 9.0 (*16*). In preparing the homology model of the ASL from *B. subtilis*, the same procedures were used as described previously (*15*), except that this time the template used was PDB 1c3u, whereas the previous model used the template PDB 1c3c (*16*), for which the *T. maritima* ASL was crystallized at pH 4.5. The only substantial difference between the two crystal structures is in the position of the imidazole of His^{68}; the structure PDB 1c3u, which is thought to represent the native enzyme, is needed for the best docking of adenylosuccinate (*16*). Because the active site is large and several substrate orientations are energetically feasible, both biochemical data and energy minimization algorithms (steepest descent followed by Polak−Ribiere conjugate gradient) were used in docking the substrate. Manipulations and energy measurements of models were achieved using the Discover 3.1 simulation program in conjunction with Insight II molecular modeling software (Biosym). A minimum of 1000 iterations was performed for each minimization.

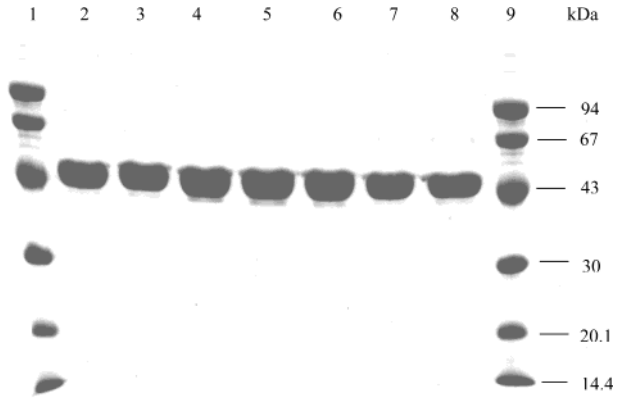

FIGURE 3: Polyacrylamide gel (12%) with 0.1% sodium dodecyl sulfate for wild-type and mutant ASLs. The contents of each lane are as follows: lanes 1 and 9, protein standards; lane 2, wild type; lane 3, Q212E; lane 4, Q212M; lane 5, N270D; lane 6, N270L; lane 7, R301K; and lane 8, R301Q. Approximately 10 μg of each enzyme was applied to the gel.

RESULTS

Activity and Purity of Gln^{212}, Asn^{270}, and Arg^{301} Mutant ASLs. Substitutions were made for the amino acid residues Gln^{212}, Asn^{270}, and Arg^{301} in ASL to determine their possible roles in catalysis. Gln^{212} was replaced by Glu (to retain side chain size/structure, while introducing a negative charge) and Met (to change residue hydrophobicity, while maintaining a similar volume); Asn^{270} was converted to Asp (to retain side chain size/structure, while introducing a negative charge) and Leu (to retain approximate residue volume, while eliminating hydrogen-bonding capability); and Arg^{301} was replaced by Lys (to retain positive charge, while changing the side-chain structure) and Gln (to retain approximate side-chain volume, while eliminating positive charge). All mutant ASL enzymes were well-expressed. As shown by 12% polyacrylamide gels containing 0.1% sodium dodecyl sulfate (Figure 3), all protein preparations were pure and the migration of both wild-type and mutant ASL enzymes was consistent with the known 50 kDa subunit molecular mass of ASL (*17*). Enzyme purity was confirmed by N-terminal sequencing.

As shown in Table 1 and its footnotes, any substitution for Gln^{212}, Asn^{270}, or Arg^{301} causes a striking decrease in catalytic activity. Therefore, these three residues are critical to the function of the enzyme. Using the spectrophotometric assay for the conversion of SAMP to AMP and fumarate, 0.0003 μmol min^{-1} mg^{-1} was the lower limit of detectable

specific activity. Only Q212E ASL, which retains the approximate size and hydrophilicity at this position, is sufficiently active to determine kinetic parameters for adenylosuccinate (Table 1). The K_m for this mutant increased only about 6-fold relative to wild-type ASL, whereas the V_{max} decreased by approximately 1000-fold. Catalytic activity is completely eliminated, however, by the substitution of Met at position 212. In this case, both the polarity and the carbonyl group of the residue side chain are absent at position 212.

Replacement of Asn at position 270 by either Asp or Leu results in extremely low to undetectable activity, consistent with this residue performing a critical role in SAMP binding and/or catalysis. Similar results were obtained for the substitution of Arg[301] by either Gln or Lys. A different positively charged residue at this position is therefore not sufficient to support enzyme function.

In addition to the conversion of SAMP to AMP and fumarate, ASL is known to catalyze a second reaction in the purine nucleotide biosynthetic pathway, the cleavage of SAICAR to produce AICAR and fumarate. Although both reactions and the structure of both substrates are similar, some human ASL mutants have been reported to exhibit unequal effects on the reactions of these two substrates (*5*, *6*). Therefore, the Gln[212], Asn[270], and Arg[301] mutants were also assayed with SAICAR. The ratio of specific activity toward SAICAR to that toward SAMP for wild-type ASL was previously reported to be near unity (*7*), and a similar ratio for the wild-type enzyme was found in the present study (0.94). However, no measurable activity (detection limit $\approx$ 0.0043 μmol min^{-1} mg^{-1}) was found for any of the mutant enzymes. The mutations apparently eliminate the ability of these enzymes to catalyze the reactions of either SAICAR or SAMP.

SAMP Binding by Mutant Enzymes. The inactive ASL mutants were tested for their ability to bind the substrate SAMP. Equilibrium binding was measured using an ultrafiltration technique, as described in the Experimental Procedures. Because the conversion of SAMP to AMP and fumarate by ASL utilizes only one substrate, mutant enzymes must be inactive to be evaluated in this way. Thus, the dissociation constants measured for Q212M, the Asn[270], and the Arg[301] mutant enzymes are best compared to the inhibition constant of the wild-type enzyme for SAMP, which acts as a competitive inhibitor with respect to AMP in the direction of SAMP formation; in that case, $K_I = 4.6$ μM (*14*). A representative Scatchard plot for Q212M ASL is shown in Figure 4.

As recorded in Table 2, each of the ASL mutants used in the present study retain the ability to bind SAMP, although with dissociation constants 7−27 times higher than the previously measured K_I for wild-type ASL (*14*). Clearly, these mutant enzymes all have a weakened affinity for the substrate. However, the low or nondetectable catalytic activity *cannot* be entirely attributed to a failure of the mutants to bind SAMP. Among these mutants, the lowest K_d was observed for Q212M ASL. R301K ASL also exhibited a relatively low K_d as compared to most of the other inactive mutants, which is not surprising given the retention of positive charge in the conversion from R to K at this position. Elimination of this charge, by mutating R301 to Q results in a further weakening of SAMP binding (higher K_d). Both of the changes at position 270 are clearly detrimental to SAMP binding. However, the higher K_d was observed in the case of N270D, in which an amino acid with a neutral, polar side chain that can participate in hydrogen bonding was replaced with a negatively charged residue.

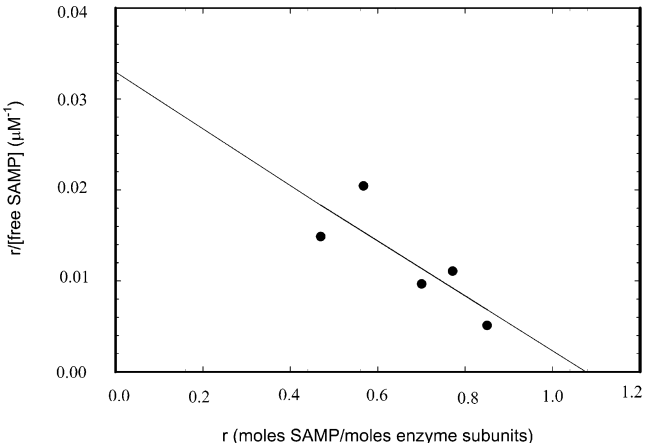

FIGURE 4: Scatchard plot for adenylosuccinate binding to the Q212M ASL mutant. The data are plotted in accordance with the Scatchard equation, $r/L_{free} = n/K_d - r/K_d$, where r is the moles of SAMP bound/mole of enzyme subunits, L_{free} is the concentration of free SAMP (in the filtrate), and K_d is the dissociation constant for the enzyme−adenylosuccinate complex. The latter value [31 ± 7 (standard error)] is calculated from the slope ($= -1/K_d$) determined by least-squares fitting of the line through the plot. Points represent averaged measurements. Experiments were conducted at room temperature in a 50 mM HEPES buffer at pH 7.

Table 2: Dissociation Constants for Adenylosuccinate[a] from Mutant Enzymes

enzyme	K_d for SAMP[b] (μM)
Q212M	31 ± 7
N270D	124 ± 11
N270L	77 ± 21
R301K	41 ± 8
R301Q	121 ± 29

[a] K_d values were determined by ultrafiltration of equilibrium mixtures of mutant enzymes and SAMP in a 50 mM HEPES buffer at pH 7 and room temperature, as described in the Experimental Procedures. [b] ± Standard deviation.

CD. CD spectra were obtained for wild-type and mutant ASL species to determine whether the secondary structure of the enzyme was altered as a result of the amino acid replacements at positions 212, 270, and 301. As shown in Figure 5, the spectrum for wild-type ASL displays pronounced minima at both 208 and 222 nm, indicating a predominance of the α-helical structure, as earlier studies of ASL have shown (*15*, *17*). Most of the mutant enzymes exhibited CD spectra that are almost identical to that of the native enzyme. This indicates that the mutations at positions 212, 270, and 301 do not substantially alter the secondary structure of the enzyme. Only the Q212M mutant exhibits evidence of some conformational change as suggested by the slight decrease in the intensities of its CD minima (Figure 5A).

Molecular Masses of Wild-Type and Mutant ASL Species. Laser-light-scattering photometry was used to determine whether the mutations in the present study affect the oligomeric state of the enzyme. Wild-type ASL has been shown to exist as an equilibrium mixture of dimeric (MW = 100 kDa) and tetrameric (MW = 200 kDa) species when

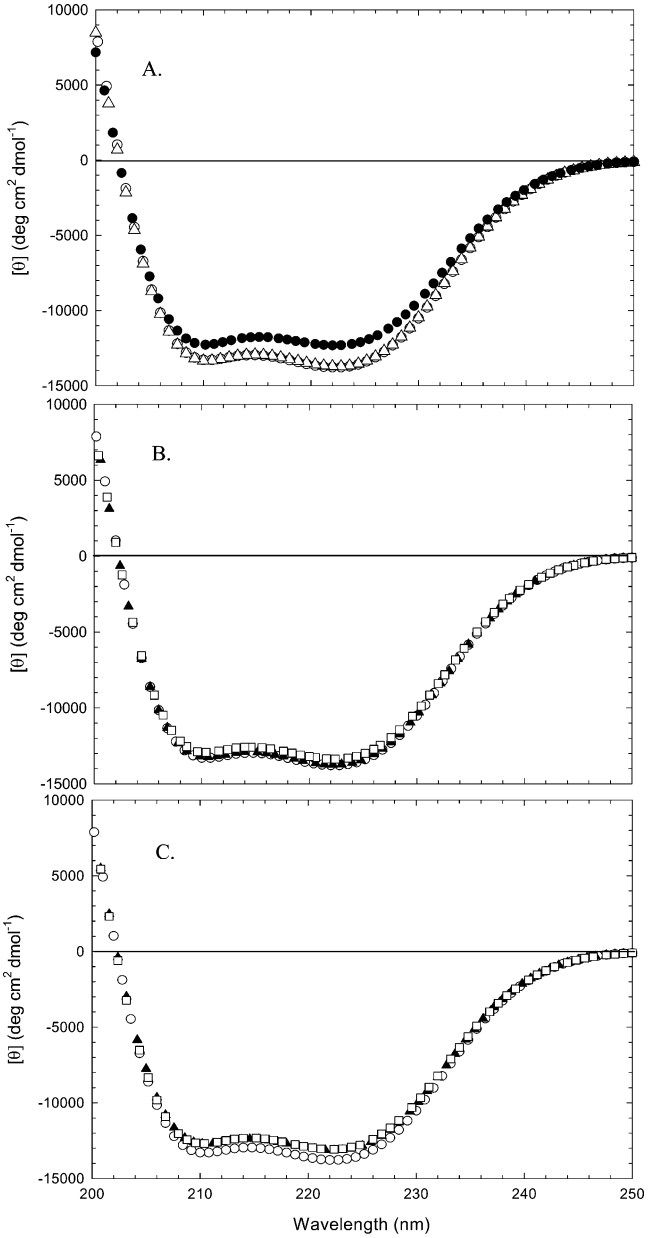

FIGURE 5: CD spectra of wild-type and mutant ASLs. Enzymes were measured at 0.3−0.6 mg/mL at room temperature in a 20 mM potassium phosphate buffer at pH 7, containing 20 mM potassium chloride. (A) Spectrum for the wild-type enzyme (○) in addition to the spectra for Q212E (△) and Q212M (●) ASL. (B) Spectra for wild-type (○), N270D (□), and N270L (▲) ASL. (C) Spectra for the wild-type enzyme (○) and the R301K (□) and R301Q (▲) mutants.

at a concentration of 0.2 mg/mL (*7*). As shown in Table 3, light-scattering measurements for wild-type ASL and each of the mutant enzymes in this study revealed similar weight average molecular masses, reflecting the presence of dimeric and tetrameric forms, with the latter predominating. Therefore, no major changes in the oligomeric state of ASL result from the mutations introduced in the present study.

Intersubunit Complementation. ASL contains four active sites per homotetramer, each of which is located at a region where three subunits come together. The mixing of two different mutant enzymes with substitutions at residues provided to the active site by different subunits results in reconstitution of some functional active sites. For a tetramer, assuming that subunits dissociate completely during mixing

Table 3: Molecular Masses of Wild-Type and Mutant ASL Species[a]

enzyme	weight average molecular mass[b] (kDa)
wild type	153 ± 5
Q212E	159 ± 1
Q212M	174 ± 17
N270D	166 ± 1
N270L	152 ± 2
R301K	173 ± 5
R301Q	219 ± 2

[a] Enzymes were measured at a concentration of approximately 0.2 mg/mL in a filtered 20 mM potassium phosphate buffer at pH 7.0, containing 20 mM potassium chloride. [b] ± Standard error.

and recombine randomly, it has been shown that $^1/_4$ of the catalytic sites should be active (*14*). This process is termed *intersubunit complementation*. Mixtures of mutants with changes at amino acids provided to the active site by the same subunit do not show an increase in activity (parts A−D of Figure 6). As illustrated in Figure 1, Asn^{270}, as well as Lys^{268} and Glu^{275} [residues previously investigated, (*15*)], is contributed to the active site by the same subunit (II, denoted in aqua); His^{141} [also identified earlier, (*14*)] is contributed by a second subunit (I, denoted in red); and Gln^{212} and Arg^{301} [in addition to the previously identified residues His^{68} (*14*) and His^{89} (*17*)] are provided by a third subunit (IV, denoted in yellow).

Although each of the mutants in the present study is severely impaired catalytically, the activities of mutants with substitutions at all three sites could be substantially activated through pairwise intersubunit complementation (Figure 6). For example, Figure 6A shows the results of mixing H68Q (with only 0.3% of wild-type activity when measured alone) with each of the seven other mutant enzymes. Up to 25% of wild-type activity was observed (e.g., with K268Q). However, H68Q did *not* exhibit activation (complementation) when combined with mutants having substitutions at residue positions 301, 89, or 212; this result indicates that each of these three residues is contributed to the active site by the same subunit as His^{68}. Figure 6B presents the results of mixing H89Q, which is only 0.2% as active as the wild-type enzyme alone, with each of the seven other mutant enzymes. Once again, substantial activation was observed for each combination, in which H89Q was mixed with an enzyme in which the mutated amino acid is provided by a different subunit (e.g., K268Q, H141Q, etc.). A similar pattern is clearly present for the combinations of various ASL mutants with the Q212E/M, R301K, and H141Q enzymes (parts C, D, and E of Figure 6, respectively). Because His^{141} is the only residue identified thus far that is provided to the active site by the subunit colored red in Figure 1, it exhibited some activation when mixed with any of the other mutant enzymes evaluated (Figure 6E). (*14*, *15*, *17*).

Among the cases in which a mixture of two mutant enzymes results in activation, it is evident that the amount of activity restored to each pair of mutants varies with regard to which residue position had been substituted on each member of the pair. Mutant enzymes with changes at positions 68, 89, 212, and 301 (subunit IV, denoted in yellow) are generally complemented somewhat more effectively by mutants with substitutions at positions 268, 270, and 275 (subunit II, denoted in blue) than by H141Q ASL

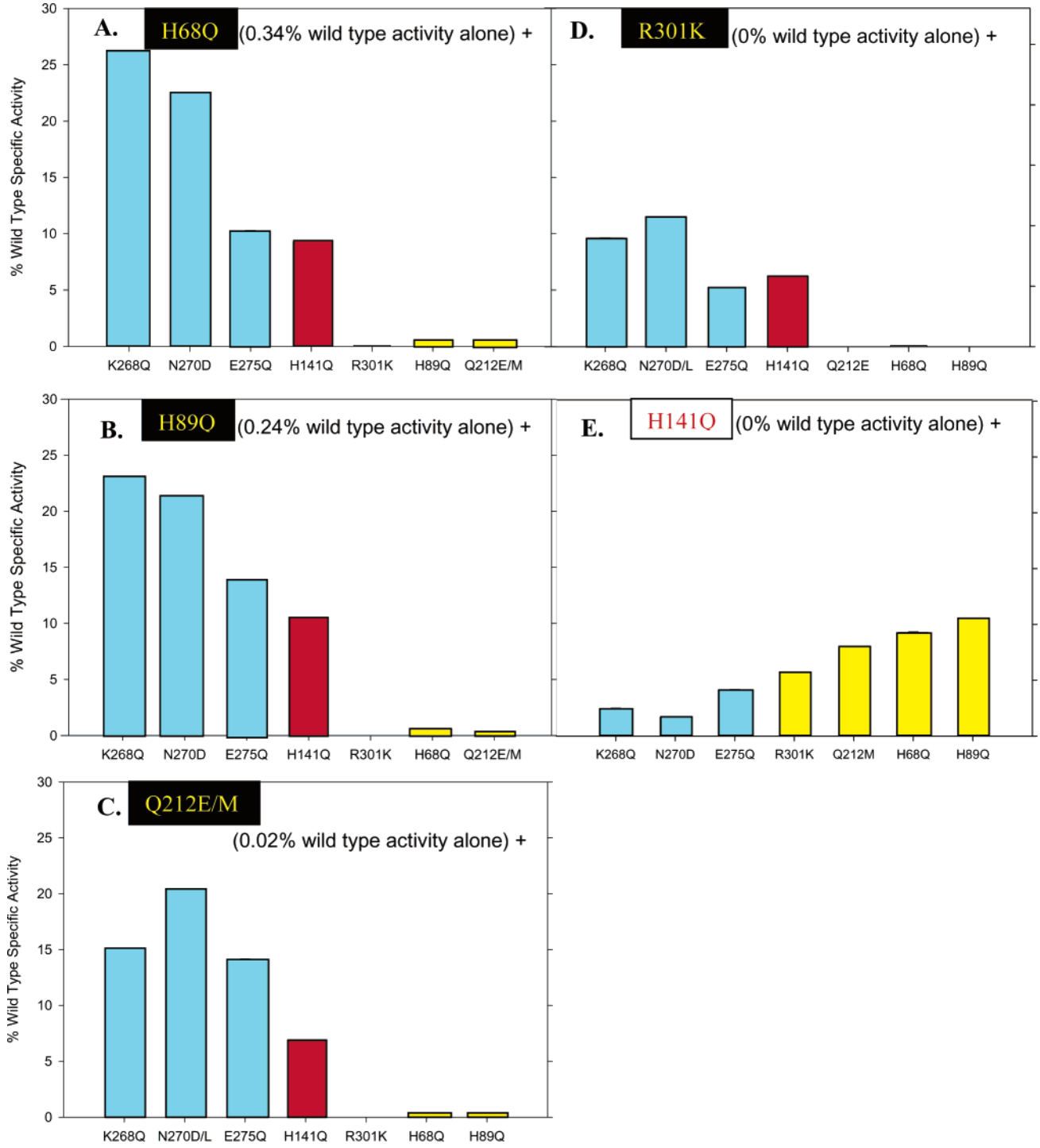

FIGURE 6: Intersubunit complementation of mutant ASLs. Pairs of mutant enzymes in a 0.1 M sodium phosphate buffer (pH 7.0) were mixed at a final concentration of 0.7 mg/mL for each, slowly frozen at −20 °C, slowly thawed at room temperature, and then incubated at 25 °C. The enzyme mixtures were assayed under standard conditions as a function of time at 25 °C until the maximum activity was reached. Bars in A−E represent maximum specific activities (expressed as a percentage of wild-type ASL activity) observed for the mixtures of each ASL mutant labeled beneath its respective bar with that indicated at the top of the panel. Thus, the activities reached when seven different mutant ASLs were each combined with the H68Q enzyme are presented in A, those obtained in combinations with H89Q ASL in B, mixtures with mutants substituted at position 212 in C, mixtures with R301K in D, and combinations with H141Q ASL in E.

(subunit I, denoted in red; parts A−D of Figure 6). However, H141Q ASL is better complemented by mutant enzymes with substitutions on the yellow subunit than by those with substitutions on the blue subunit (Figure 6E). Furthermore, E275Q ASL consistently exhibited less reactivation when combined with mutants at yellow subunit positions than did K268Q or N270D(L), even though the three residues are contributed to the active site by the same subunit (denoted in blue; parts A−D of Figure 6). Similarly, R301K ASL exhibited a lower ability (than other mutants on the same yellow subunit) to complement any of the other mutant ASLs (parts A−E of Figure 6).

DISCUSSION

In the present study, the catalytic roles of active-site residues Gln[212], Asn[270], and Arg[301] of ASL were probed by

Table 4: Interatomic Distances (Å) between SAMP and Active-Site Residues of ASL

		enzymes						
atom 1	atom 2	wild type	Q212E	Q212M	N270D	N270L	R301K	R301Q
Q212−N[a]	SAMP α-COO$^-$ [b]	3.07	**6.90**	**4.39**	3.32	3.11	3.49	**3.68**
N270−N[a]	SAMP β-COO$^-$ [b]	2.85	2.87	2.82	**5.87**	**3.37**	2.94	2.82
R301−N[a]	SAMP α-COO$^-$ [b]	3.58	**5.10**	**4.63**	3.11	3.30	**2.75**	**5.05**
K268−N	SAMP−OPO_3	4.46	**3.82**	4.31	4.40	4.04	4.18	4.30
H68−ϵN	SAMP β-COO$^-$ [b]	3.41	3.02	3.03	**2.83**	3.62	**2.88**	**2.88**
H89−δN	SAMP ribose 2′O	4.91	**3.91**	**4.23**	4.78	5.14	5.04	**4.09**
H141−ϵN	SAMP β-C	3.36	3.64	**3.96**	3.47	3.37	3.31	3.85

[a] In mutant enzymes, the distances given are the closest between the side chain and atom 2. [b] α-COO$^-$ and β-COO$^-$ of the succinyl moiety of SAMP are the same as those designated in the caption of Figure 1.

site-directed mutagenesis. Gln[212] and Asn[270] were previously pointed out by Toth and Yeates (*16*), in describing the crystal structure, as potential hydrogen-bond donors to the carboxylate anions of adenylosuccinate based on their proximity to this substrate when docked into the active site of the *T. maritima* ASL crystal structure (Figure 1). Arg[301] is also found in the same region of the active site and could interact with the carboxylate groups on the substrate electrostatically, as illustrated in Figure 1. Mutant enzymes were constructed containing either Glu or Met in place of Gln[212], Asp or Leu in place of Asn[270], and Gln or Lys in place of Arg[301]. The results show that each of these mutations reduced enzyme-specific activities toward both SAMP and SAICAR to extremely low levels (1000- to at least 5000-fold reduction). Binding studies for most of the mutant enzymes revealed decreases in binding affinity for adenylosuccinate of 7−27-fold, as compared with the wild type. In addition, Q212E ASL showed a K_m for SAMP that is six times that of the wild-type enzyme. Although the predominant effect of the mutations is a severely decreased catalytic rate, it is evident that SAMP affinity is substantially weakened in these mutant enzymes. Earlier work has suggested that interaction of the succinyl portion of SAMP with the enzyme active site provides the majority of the binding energy for this substrate (*17*). Hence, it is not surprising that changing any of the amino acids of the enzyme within binding distance of the succinyl carboxylate groups has a major effect on the enzyme function. Weakened binding probably indicates altered binding, in which the substrate is not optimally oriented for the catalytic reaction.

The CD spectra of most of the mutant enzymes are superimposable onto that of the wild-type enzyme; only the Q212M enzyme exhibited a minor change in its CD spectrum. Hence, the catalytic deficits of these enzymes cannot be attributed to the change in secondary structure. In addition, no substantial changes in the enzyme oligomeric state resulted from the mutations. A recent study suggested a direct relationship between the catalytic activity of the enzyme and the proportion of ASL present in the tetrameric, as opposed to dimeric, state (*7*). Because the mutant enzymes in the present study do not differ appreciably from the wild-type enzyme in weight average molecular mass, the effects on ASL activity *cannot* be explained by a shift in the subunit association−dissociation equilibrium.

To better understand the effects of these mutations, a homology model was used in which SAMP was docked into the active site of the wild-type enzyme. Unlike previous studies, which utilized a model based on a structure of ASL from *T. maritima* that was crystallized at pH 4.5 (PDB 1c3c, *16*), the model presently used was based on an X-ray structure of *T. maritima* ASL that was crystallized at pH 9.0 (PDB 1c3u), a condition at which this enzyme is active (*16*). Figure 1 depicts key residues of the wild-type ASL active site, including those that are the subject of the current work, in the presence of docked SAMP. Prior to energy minimization of the model to obtain this figure, SAMP was aligned in the active site in accordance with the most recent biochemical data so that the appropriate regions of this substrate were within suitable distance of His[68] and His[141] for these residues to perform their previously identified roles of general acid and base, respectively (*14*, *20*, *21*). After minimization of this structure, however, His[68] was no longer within hydrogen-bonding distance of either N1 or N6 of SAMP (the distance between N6 and the closest nitrogen on the imidazole ring of His[68] increased to greater than 4 Å) but was instead poised to interact at short range with one of its four succinyl carboxylate oxygens (Figure 1). The implication is that the protonated form of His[68] may contribute to the binding of adenylosuccinate by the enzyme. It was previously reported for the mutant H68Q that, in addition to exhibiting a V_{max} that is decreased 100-fold, the K_m for adenylosuccinate is almost four times that of the wild-type enzyme (*21*). However, the crystal structure of the *T. maritima* enzyme indicates that there is a water molecule close to the ϵN of His[68], which in the model would be close to N6 of SAMP. We therefore propose that, in addition, His[68] polarizes this water molecule, which serves as the general acid by donating a proton to the N6 of SAMP. Because this function of His[68] would also require its existence in the protonated state, the participation of this residue in substrate binding may additionally contribute to stabilizing its cationic form. Through a similar comparison to the structure of the *T. maritima* enzyme, a separate water molecule had previously been implicated in mediating the hydrogen-bonding interaction between His[89] of *B. subtilis* ASL and the 2′-OH of the ribose moiety on adenylosuccinate (*15*).

According to Figure 1, which depicts the energy-minimized model of wild-type ASL, and the interatomic distances (determined from this model) listed in the first row of Table 4, Gln[212], Asn[270], and Arg[301], as well as Arg[67] and His[68], are strongly implicated in coordinating the carboxylate anions of SAMP through hydrogen-bonding and electrostatic interactions with this substrate. In addition to the likely role of Arg[301] in SAMP binding, the ϵ-guanidinium group of Arg[301] is also sufficiently close to the ϵ nitrogen of the imidazole ring of His[141] (3.67 Å) that the presence of its positive charge could result in a lowering of the p*K* of the His[141] side chain, thereby improving the ability of this residue

to function as a general base. The difference in its side-chain structure may render lysine at position 301 to be ineffective for this function. The proximity of the succinyl moiety of SAMP to this positively charged residue, as well as to His[68] in the protonated state, may also stabilize the putative carbanion generated in this part of the SAMP molecule following removal of one of the β protons by the general base. The implication of positively charged residues performing this role has previously been proposed for other members of the superfamily: *E. coli* fumarase C (*30*) and turkey δ crystallin (*31*).

To model the amino acid substitutions at positions 212, 270, and 301 of ASL, these residues were individually replaced in the *B. subtilis* ASL active-site structure shown in Figure 1. The models of these mutant enzymes were then subjected to the same energy-minimization procedures used for the wild-type enzyme model. Figure 7 shows the effects of the representative changes Q212M, N270D, and R301Q (A, B, and C of Figure 7, respectively) on the orientations of key amino acid residues in the active site by overlaying the energy-minimized models of each of these mutant enzymes onto that of wild-type ASL (SAMP was omitted from this figure for clarity but was included in the modeling). These figures depict mostly minor changes in the positions of identified active-site amino acids as a result of each mutation, consistent with little or no changes in the overall enzyme structure suggested by CD spectroscopy.

Table 4 lists the distances between specific atoms on SAMP and specific atoms of the enzyme active-site residues that underwent the greatest changes in response to the mutations for the wild-type and mutant enzymes. Inspection of this table reveals similar values between the wild-type and each of the mutant enzymes for many of the distances measured. For the Q212E mutant, however, the distance from one of the oxygens of the α carboxylate of SAMP to the nearest atom on the replacement Glu residue is more than doubled as compared with the distance from this oxygen to Gln[212] in the wild-type enzyme, presumably as a result of electrostatic repulsion between two negatively charged groups. As Table 4 indicates, distances between SAMP and other residues in this mutant vary, both positively and negatively, with regard to the corresponding distances in the wild-type enzyme. Perhaps the distances that became smaller with respect to those of the wild-type enzyme (e.g., from the 2′ ribose OH group of SAMP to His[89]), partially compensate for those that became larger, accounting for the higher activity of the Q212E mutant as compared to the others. When Gln[212] is exchanged for Met at this position, substituting a nonpolar side chain for one that is polar and capable of hydrogen bonding, the distance between the α-carboxylate oxygen and its nearest atom on Met[212] is also substantially larger than the corresponding distance in wild-type ASL but not as great as that of the Q212E enzyme. Similarly, the distance between an oxygen atom of the β-carboxylate group of SAMP and its nearest atom on the residue at position 270 is greatly increased when Asp (N270D) is substituted in this position (also because of the probable electrostatic repulsion) and only slightly increased when nonpolar leucine is substituted (N270L). Changing Arg[301] to Gln (R301Q) increases the distance between this residue and the SAMP carboxylate oxygen to which it is closest, but Lys in this position (R301K) results in a decrease

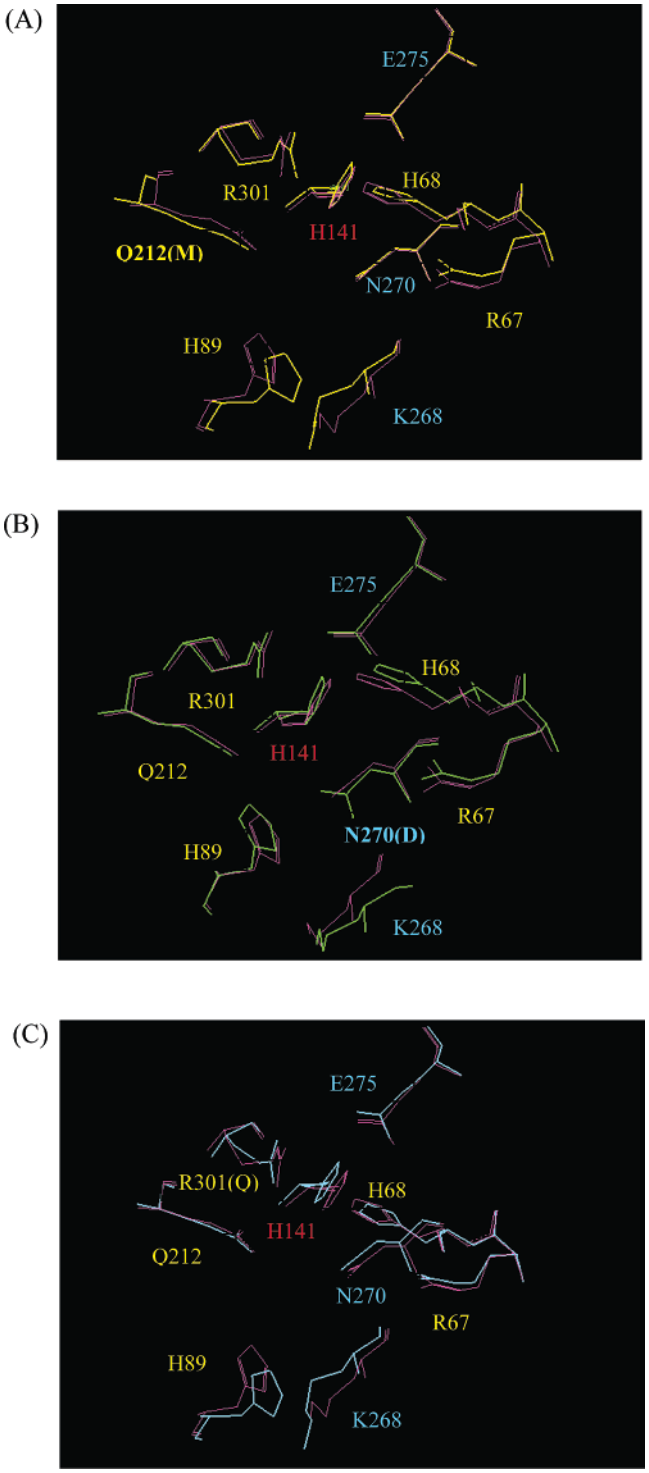

FIGURE 7: Energy-minimized models depicting amino acids in wild-type ASL overlaid with those of the (A) Q212M, (B) N270D, and (C) R301Q mutant enzymes. In A, residues from the wild-type enzyme are colored pink and those from the Q212M mutant are colored yellow. In B, wild-type residues are colored pink and N270D ASL residues are colored bright green. In C, wild-type residues are colored pink and those from R301Q ASL are colored cyan.

in the distance of similar magnitude. Aside from the distances between the carboxylate groups of SAMP and the enzyme residues that were substituted, some indirect distance changes also occurred as a result of the mutations. For example, both of the Gln[212] substitutions result in a lengthening of the distance between SAMP and Arg[301], possibly attributable to

the proximal location of these two residues and their origin from a common subunit (see Figure 1). This explanation may also apply to the indirect effects of interchanges at positions 301 or 212 on distances from SAMP to both His^{68} and His^{89} (Table 4). Nonetheless, each of the distances shown in this table appears to be important for the enzyme function, in that the loss of activity does not appear to correlate with a change in any one particular interatomic distance; variation in any one or more of these may underlie the activity loss. Figure 1 depicts multiple possible interactions between the succinyl carboxylate groups of SAMP and active-site residues of wild-type ASL. The loss of any of these interactions, which presumably occurs as a result of each of the amino acid replacements, would be expected to affect the binding affinity or orientation of SAMP in the active site. Because the decreases in binding affinities measured in the present study are significant, though not commensurate with the activity losses toward this substrate, it is probable that the present mutations result in a decrease in the ability of the enzyme to optimally orient its substrates for catalysis. Only the structure of SAMP, and not that of SAICAR, was used in the present modeling studies, although both of these substrates are very similar in structure and undergo the same reaction. It is therefore likely that both bind similarly to the enzyme active sites.

Intersubunit Complementation. The ability of two inactive mutant enzymes with substitutions at residue positions contributed to the active site by two different subunits to mutually compensate each other for the loss of function, resulting in an enzyme activation, confirms the importance of each of these specific residues as critical participants in the intersubunit active site and/or catalytic mechanism of the enzyme. Mutants of ASL (*14*, *15*, *17*, *32*, *33*), as well as other members of the fumarase superfamily (*34*), have been shown to exhibit such intersubunit complementation. Using this approach, it was determined that each active site of ASL contains different regions of three separate subunits (*15*). Overall, the results of the complementation studies presented here strongly support the idea that the loss of enzyme function in connection with the mutations produced at positions 212, 270, and 301 of ASL were caused by the specific replacement of three functionally critical amino acids with others that are unable to perform the same roles. This is evident in the observation that each of the mutant enzymes, assayed in these studies, combined with another ASL single-site mutant enzyme with a replacement from a different subunit, exhibited a gain in specific activity.

Nevertheless, variation has been reported in the relative amount of activation observed among pairs of ASL mutants assayed (*15*, *17*). In this study, we have found that mixtures of enzymes with mutations at active-site residues contributed by the yellow (IV) and blue (II) subunits show higher levels of activation than mixtures with substitutions at residues from the yellow (IV) and red (I) subunits. The least activation was observed for mixtures with red (I) and blue (II) subunit substitutions. These data are consistent with the structure of the ASL tetramer previously proposed in which the red/yellow and blue/yellow subunit interfaces both have greater areas than the red/blue subunit interface (Figure 8). Because the interfacial regions of a multimeric enzyme comprising larger areas should be more resistant to local changes than those containing smaller areas, substitution of a single amino

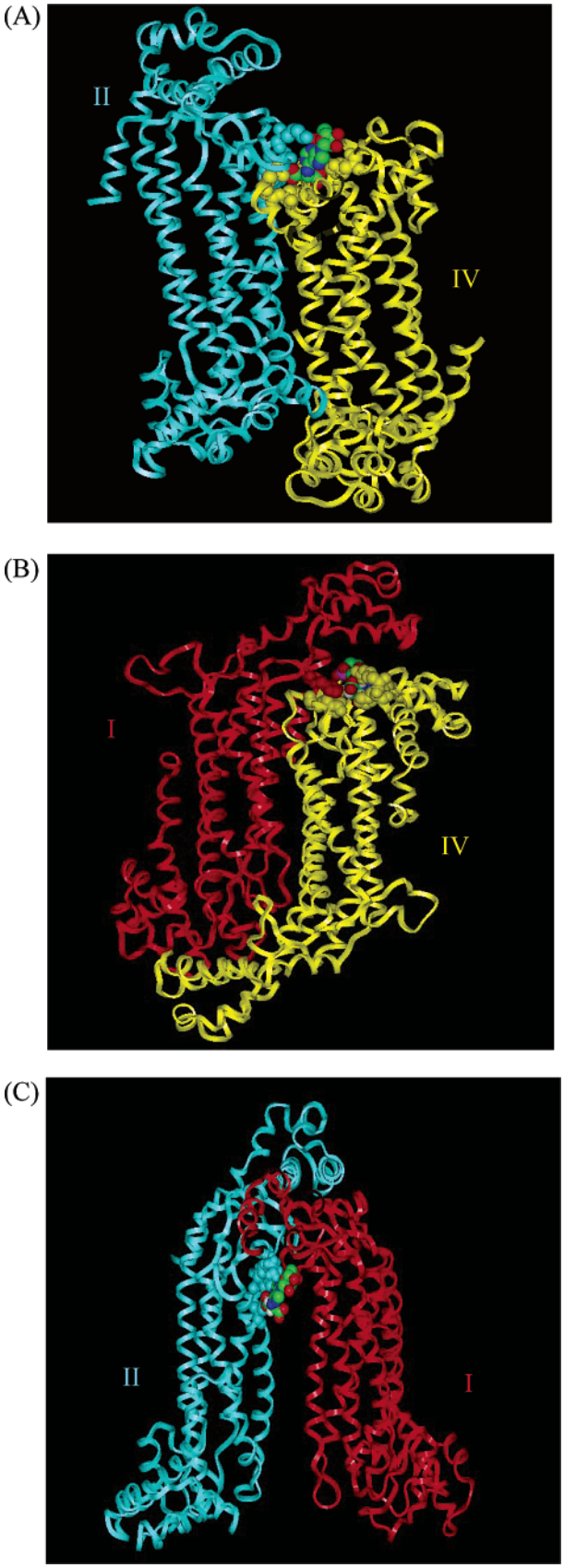

FIGURE 8: Interfaces between pairs of subunits in wild-type ASL. (A) Subunits II (aqua) and IV (yellow). (B) Subunits I (red) and IV (yellow). (C) Subunits I (red) and II (aqua). SAMP and active-site amino acid residues are shown in space-filling form. SAMP is colored according to the atom, and the enzyme residues are colored to match their subunits of origin. The subunits were numbered according to ref *15* for the purpose of consistency.

acid at a red/blue subunit interface region may be sufficient to markedly alter subunit interactions. His[141] is the only residue identified thus far that has contributed to the functional active site of ASL from the red (I) subunit. Substitution of this residue may therefore reduce the ability of the mutated subunit to reassociate with other subunits following experimentally induced dissociation or promote incorrect association, resulting in a distorted active-site structure and lower catalytic activity. This could also explain why this mutant enzyme combined with an enzyme with a yellow subunit mutation did not exhibit as much activation as a yellow/blue mutation mixture even though the interfacial area is similarly large.

Of the residues originating from the yellow subunit (IV), R301K ASL exhibited the least activation when mixed with any other mutant enzyme. It had been previously suggested that, while activation is limited by the ability of subunits to reassociate in the case of mixed mutant enzymes bearing mutations on the red (I) and blue (II) subunits, dissociation of subunits bearing the same mutation is the limiting factor among combinations of red (I)/yellow (IV) or blue (II)/yellow (IV) mutant subunits (*15*). Because it is close to both Glu[275] and His[141], Arg[301] is present at the interface of the two other subunits that make up the active site (Figure 1). It is therefore possible that exchanging the Arg residue at this position for Lys, an amino acid with a less bulky side chain, facilitates interaction among subunits so that they dissociate less readily. The same explanation may apply for intersubunit complementation involving the E275Q enzyme because, of the three identified active-site amino acids originating from the blue subunit, ASL mutated at position 275 exhibited the least activation when mixed with other mutant enzymes.

The present work indicates that Gln[212], Asn[270], and Arg[301] each perform critical functions in catalysis by ASL through their contributions to the binding and orientation of the succinyl carboxylate groups on its two substrates SAICAR and SAMP. Asn[270] most likely hydrogen-bonds to the closest oxygen on the β-carboxylate group of the substrate, Gln[212] hydrogen-bonds to the closest α-carboxylate oxygen, and Arg[301] probably interacts electrostatically with the other α-carboxylate oxygen (Figure 1). Furthermore, the position of Arg[301] suggests possible roles in catalysis, such as stabilizing the carbanion intermediate that results from proton abstraction from the substrate by His[141], or modulating the pK_a of the imidazole side chain of this residue. Although substrate binding is significantly affected by mutations at these three sites, the major effect of each is a severe loss in the catalytic function. As revealed by computer modeling of docked SAMP, in addition to the loss of groups directly involved in coordination of the SAMP carboxylate anions, the mutations influence distances between various other residues on the enzyme and the atoms on SAMP with which they putatively interact (Table 4). This suggests that the loss in enzyme activity is likely due to various perturbations in substrate orientation that differ from one mutant enzyme to another.

ACKNOWLEDGMENT

The authors wish to thank Jennifer Brosius Palenchar for her assistance in these studies and for the homology model of *B. subtilis* ASL based on the crystal structure of *T. maritima* ASL (PDB 1c3u) at pH 9.0 and Yan He for her assistance with the figures. We thank Dr. Yu Chu Huang for determining the amino terminal sequences of the wild-type and mutant enzymes.

NOTE ADDED AFTER ASAP POSTING

An earlier version of this paper posted to the ASAP website on May 21, 2004, contained two errors. K_m values of wild-type ASL for SAMP and SAICAR (in paragraph 5 of Experimental Procedures) had incorrect units and an author in ref 23 should have been deleted. These instances have been corrected in this new version posted May 24, 2004.

REFERENCES

1. Ratner, S. (1972) Argininosuccinases and adenylosuccinases, in *The Enzymes* (Boyer, P. D., Ed.) 3rd ed., Vol. 7, pp 167−197, Academic Press, New York.
2. Jaeken, J., and Van Den Berghe, G. (1984) An infantile autistic syndrome characterized by the presence of succinylpurines in body fluids, *Lancet 2*, 1058−1061.
3. Jaeken, J., Wadman, S. K., Duran, M., van Sprang, F. J., Beemer, F. A., Holl, R. A., Theunissen, P. M., de Cock, P., van den Bergh, F., Vincent, M. F., and van den Berghe, G. (1988) Adenylosuccinase deficiency: An inborn error of purine nucleotide synthesis, *Eur. J. Pediatr. 148*, 126−131.
4. Marie, S., Cuppens, H., Heuterspreute, M., Jaspers, M., Tola, E. Z., Gu, X. X., Legius, E., Vincent, M., Jaeken, J., Cassiman, J., and Van den Berghe, G. (1999) Mutation analysis in adenylosuccinate lyase deficiency: Eight novel mutations in the reevaluated full ADSL coding sequence, *Hum. Mutat. 13*, 197−202.
5. Race, V., Marie, S., Vincent, M., and Van den Berghe, G. (2000) Clinical, biochemical, and molecular genetic correlations in adenylosuccinate lyase deficiency, *Hum. Mol. Genet. 9*, 2159−2165.
6. Van den Berghe, G., and Jaeken, J. (2001) Adenylosuccinate lyase deficiency, in *The Metabolic and Molecular Basis of Inherited Diseases* (Scriver, C. R., Beaudet, A. L., Sly, W. S., Valle, D., Childs, B., Kinzler, K. W., and Vogelstein, B., Eds.) 8th ed., Vol. 2, pp 2653−2662, McGraw−Hill, New York.
7. Palenchar, J. B., and Colman, R. F. (2003) Characterization of a mutant *Bacillus subtilis* adenylosuccinate lyase equivalent to a mutant enzyme found in human adenylosuccinate lyase deficiency: Asparagine 276 plays an important structural role, *Biochemistry 42*, 1831−1841.
8. Palenchar, J. B., Crocco, J. M., and Colman, R. F. (2003) The characterization of mutant *Bacillus subtilis* adenylosuccinate lyases corresponding to severe human adenylosuccinate lyase deficiencies, *Protein Sci. 12*, 1694−1705.
9. Weaver, T. M., Levitt, D. G., Donnelly, M. I., Wilkens Stevens, P. P., and Banaszak, L. J. (1995) The multisubunit active site of fumarase C from *Escherichia coli*, *Nat. Struct. Biol. 2*, 654−662.
10. Shi, W., Dunbar, J., Jayasekera, M. M. K., Viola, R. E., and Farber, G. K. (1997) The structure of L-aspartate ammonia-lyase from *Escherichia coli*, *Biochemistry 36*, 9136−9144.
11. Sampaleanu, L. M., Vallée, F., Thompson, G. D., and Howell, P. L. (2001) Three-dimensional structure of the argininosuccinate lyase frequently complementing allele Q286R, *Biochemistry 40*, 15570−15580.
12. Yu, B., and Howell, P. L. (2000) Intragenic complementation and the structure and function of argininosuccinate lyase, *Cell. Mol. Life Sci. 57*, 1637−1651.
13. Simpson, A., Bateman, O., Driessen, H., Lindley, P., Moss, D., Mylvaganam, S., Narebor, E., and Slingsby, C. (1994) The structure of avian eye lens δ-crystallin reveals a new fold for a superfamily of oligomeric enzymes, *Nat. Struct. Biol. 1*, 724−734.
14. Lee, T. T., Worby, C., Bao, Z., Dixon, J. E., and Colman, R. F. (1999) His[68] and His[141] are critical contributors to the intersubunit catalytic site of adenylosuccinate lyase of *Bacillus subtilis*, *Biochemistry 38*, 22−32.

15. Brosius, J. L., and Colman, R. F. (2002) Three subunits contribute amino acids to the active site of tetrameric adenylosuccinate lyase: Lys^{268} and Glu^{275} are required, *Biochemistry 41*, 2217−2226.
16. Toth, E. A., and Yeates, T. O. (2000) The structure of adenylosuccinate lyase, an enzyme with dual activity in the *de novo* purine biosynthetic pathway, *Structure 8*, 163−174.
17. Brosius, J. L., and Colman, R. F. (2000) A key role in catalysis for His^{89} of adenylosuccinate lyase of *Bacillus subtilis*, *Biochemistry 39*, 13336−13343.
18. Bridger, W. A., and Cohen, L. H. (1968) The kinetics of adenylosuccinate lyase, *J. Biol. Chem. 243*, 644−650.
19. Hanson, K. R., and Havir, E. A. (1972) The enzymic elimination of ammonia, in *The Enzymes* (Boyer, P. D., Ed.) 3rd ed., Vol. 7, pp 75−166, Academic Press, New York.
20. Lee, T. T., Worby, C., Dixon, J. E., and Colman, R. F. (1997) Identification of His^{141} in the active site of *Bacillus subtilis* adenylosuccinate lyase by affinity labeling with 6-(4-bromo-2,3-dioxobutyl)thioadenosine 5′-monophosphate, *J. Biol. Chem. 272*, 458−465.
21. Lee, T. T., Worby, C., Bao, Z., Dixon, J. E., and Colman, R. F. (1998) Implication of His^{68} in the substrate site of *Bacillus subtilis* adenylosuccinate lyase by mutagenesis and affinity labeling with 2-[(4-bromo-2,3-dioxobutyl)thio]adenosine 5′-monophosphate, *Biochemistry 37*, 8481−8489.
22. Segall, M. L., and Colman, R. F. (2003) Gln^{212}, Asn^{270}, and Arg^{301} are critical for catalysis by adenylosuccinate lyase, *Biochemistry 42*, 8614.
23. Redinbo, M. R., Eide, S. M., Stone, R. L., Dixon, J. E., and Yeates, T. O. (1996) Crystallization and preliminary structural analysis of *Bacillus subtilis* adenylosuccinate lyase, an enzyme implicated in infantile autism, *Protein Sci. 5*, 786−788.
24. Laemmli, U. K. (1970) Cleavage of structural proteins during the assembly of the head of Bacteriophage T4, *Nature 227*, 680−685.
25. Tornheim, K., and Lowenstein, J. M. (1972) The purine nucleotide cycle: The production of ammonia from aspartate by extracts of rat skeletal muscle, *J. Biol. Chem. 247*, 162−169.
26. Woodward, D. O., and Braymer, H. D. (1966) Purification and properties of *neurospora* adenylosuccinase, *J. Biol. Chem. 241*, 580−587.
27. Bradford, M. M. (1976) A rapid and sensitive method for the quantitation of microgram quantities of protein utilizing the principle of protein-dye binding, *Anal. Biochem. 72*, 248−254.
28. Wyatt, P. J. (1993) Light scattering and the absolute characterization of macromolecules, *Anal. Chim. Acta 272*, 1−40.
29. Chilson, O. P., Costello, L. A., and Kaplan, N. O. (1965) Effects of freezing on enzymes, *Fed Proc. 24*, S55−S65.
30. Weaver, T., and Banaszak, L. (1996) Crystallographic studies of the catalytic and a second site in fumarase C from *Escherichia coli*, *Biochemistry 35*, 13955−13965.
31. Simpson, A., Bateman, O., Driessen, H., Lindley, P., Moss, D., Mylvaganam, S., Narebor, E., and Slingsby, C. (1994) The structure of avian eye lens δ-crystallin reveals a new fold for a superfamily of oligomeric enzymes, *Nat. Struct. Biol. 1*, 724−734.
32. Woodward, D. O., Partridge, C. W. H., and Giles, N. H. (1958) Complementation at the AD-4 locus in *Neurospora crassa*, *Proc. Natl. Acad. Sci. U.S.A. 44*, 1237−1244.
33. Woodward, D. O. (1959) Enzyme complementation in vitro between adenylosuccinaseless mutants of *Neurospora crassa*, *Proc. Natl. Acad. Sci. U.S.A. 45*, 846−850.
34. Turner, M. A., Simpson, A., McInnes, R. R., and Howell, P. L. (1997) Human argininosuccinate lyase: A structural basis for intragenic complementation, *Proc. Natl. Acad. Sci. U.S.A. 94*, 9063−9068.

BI0494774